International Journal of the Physical Sciences Vol. 5(6), pp. 781-792, June 2010
Available online at http://www.academicjournals.org/IJPS
ISSN 1992 - 1950 ©2010 Academic Journals

Full Length Research Paper

Modeling of pre-cast concrete hybrid connections by considering the residual deformations

Sevket Ozden[1]* and Onur Ertas[2]

[1]Department of Civil Engineering, Kocaeli University, Kocaeli, Turkey.
[2]OTS Construction, Engineering, Architecture and Consultancy Co., Istanbul, Turkey.

Accepted 14 April, 2010

This paper presents an alternative section analysis and hysteretic modeling for the response of pre-cast concrete hybrid connections which have different level of mild steel contributions to the connection flexural capacity. Well-known classical reinforced concrete section analysis approaches cannot be directly applied to the pre-cast concrete hybrid connections due to the strain incompatibility between the concrete section, and the partially bonded mild steel, and the un-bonded pre-stressing tendons. In the proposed section analysis, initially the moment-rotation behavior of the hybrid connection is modeled by providing a new de-bonding length formulation for the mild steel. Later, a hysteretic response model is proposed by considering the residual displacements measured during the hybrid connection subassembly tests. The general trends and the energy dissipation predictions of the proposed model are compared with the previously published reversed cyclic test results. It is observed that the proposed moment-rotation envelope model and the cyclic response behavior model both exhibit satisfactory agreement with the previously published test results.

Key words: Precast concrete, post-tensioning, hybrid connections, moment-rotation envelope, de-bonding length, residual deformations, hysteretic modeling.

INTRODUCTION

The design and performance of post-tensioned connections of precast reinforced concrete members have attracted considerable attention in the last two decades. The self-centering ability of such structures, along with the high lateral nonlinear displacement capability with minimum damage to the framing members may be highlighted as the reasons of increasing popularity on so called “hybrid connections”. Various types of post-tensioning applications were reported on concrete or steel moment resisting frames (MRF) and precast concrete walls and bridge piers (Kurama, 2002; Kwan and Billington, 2003; Ozden and Ertas 2007; Priestley and MacRae, 1996; Ricles et al., 2002; Stone et al., 1995). Extensive experimental and analytical research on the seismic performance of hybrid connections (Nakaki, 1999; Priestley et al., 1999) resulted in design guidelines (ACI T1.02-03-2003) for this relatively new construction practice.

*Corresponding author. E-mail: sevketozden@yahoo.com.

The section analysis, namely moment and displacement capacity predictions, and the hysteretic behavior of post-tensioned connections are widely different than that of the conventional reinforced concrete or steel members, due to the strain incompatibility throughout the member cross section under a given rotation. Many investigations on numerical approaches for performance calculations were reported in the literature for post-tensioned steel or precast MRF’s and precast walls (Cheok et al., 1998; Christopoulos et al., 2002a; Christopoulos et al., 2002b; Christopoulos et al., 2003; El-Sheikh et al., 2000; El-Sheikh et al., 1999; Kurama, 2000; Kurama, 2001; Kurama et al., 1999, Pampanin et al., 2001; Priestley and Tao, 1993; Ricles et al., 2001).

An experimental and numerical research on the performance of hybrid connections with varying mild steel content was carried out at Bogazici and Kocaeli Universities in Turkey and funded by the Scientific and Technical Research Council of Turkey (TUBITAK-Project No: ICTAG I589) and the Turkish Precast Association. Within the content of this piece of work presented here, a section analysis for hybrid connections with bond-slip

response of mild steel and an alternative hysteretic model by considering the residual deformations are presented.

LITERATURE SURVEY

In the theoretical background for the current modeling of post-tensioned connections of the precast concrete moment resisting frames, the fundamentals of the currently available models need to be discussed. Firstly, a simple tri-linear idealization of the force-displacement response of unbonded post-tensioned connections was developed by Priestly and Tao (1993). There were three key points in the definition of the response curve. They were the decompression point, the linear limit for the section and the proportionality limit of the post-tensioning steel. The first point on the curve was defined as the precompression stress on the extreme fiber of the section and it was assumed that the flexural cracks start to propagate when this stress was lost. The second point was the end of the elastic behavior. The last point was the limit of proportionality on the steel stress-strain curve, since it was reasonable to assume at this stage that concrete ultimate conditions were approached (Priestley and Tao, 1993).

Secondly, a parametric study was performed by Cheok et al. (1998), about the hybrid connections by using the program IDARC (Kunnath et al., 1992) which is capable of nonlinear structural analysis. The proposed model was characterized by seven unique feature parameters that were developed from experimental observations. Hysteretic parameters were identified for five different connection types. The parameters were calibrated using the experimental load-deformation data which was scaled using similitude requirements to account for the reduced scale of test specimens.

Another study about modeling the post-tensioned precast concrete connections was reported by El-Sheikh (El-Sheihk et al., 1999; El-Sheikh et al., 2000). That study was based on a spring and fiber approach modelled in DRAIN-2DX (Prakash et al., 1993) software. In the content of this model, limit state points were defined. The first point was the estimation of the linear behavior limit. The linear limit moment was considered to be the smaller of the two values; the first value accounts for concrete softening and the second value accounts for the geometric softening due to the gap opening. The linear limit rotation was calculated assuming the beam was uncracked. The second point was defined by the yield limit state with several assumptions, as listed below:

(1) The elastic flexural deformations over the length was negligible
(2) The center of rotation at the beam-column interface was at the neutral axis
(3) The cover concrete was spalled.

The last point of the moment-rotation curve defined by El-Sheikh (El-Sheihk et al., 1999; El-Sheikh et al., 2000) was the estimation of the ultimate limit state. In this state, the ultimate moment was equal to the yield moment and the ultimate rotation capacity was calculated from the ultimate strain of the confined concrete and from the critical failure length.

The modeling of the unbonded post-tensioned connections with mild steel was discussed by Pampanin in 2001 (Pampanin et al., 2001). The reported model provides an iterative section analysis method, incurporating an analogy with equivalent cast-in-place beam and named as “monolithic beam analogy”, and additional conditions applied on the member global displacements. A similar approach was presented for post-tensioned steel frame connections by Christopoulos in 2002 (Christopoulos et al., 2002b).

The flag-shaped model and its hysteretic rules were defined by Christopoulos for self-centering post-tensioned connections in 2002 (Christopoulos et al., 2002a). In this model, loading, unloading and reloading stiffness values were defined and a parametric study about post-yield stiffness and energy dissipation characteristics were presented. The details of flag-shaped behavior will be discussed in the cyclic modeling part of this paper.

PROCEDURE FOR MOMENT-ROTATION ANALYSIS

In the previous part of this paper, the behavior of hybrid connections and some of the available numerical approaches are summarized. The complexity of the section analysis of unbonded post-tensioned connections may easily be pointed out from the available literature since the classical analysis procedures of monolithic reinforced concrete for moment-curvature relationship is not directly applicable. In this part of the study, definition of moment-rotation behavior of post-tensioned sections with mild steel will be discussed.

The hybrid connection concept is defined as the existence of unbonded strands in the mid-depth of the beam crossection and mild steel on the top and bottom of the beam with partially unbonded lengths as defined in ACI-T1.2-03 (ACI-T1.2-03, 2003). For the analysis of such type of connections, a simple and iterative procedure for the equilibrium equations was previously defined by Pampanin (Pampanin et al., 2001). The current procedure for the response envelope is based on this approach with a modification of new debonding length estimation formula for the partially bonded mild steel. Besides, as a new development, the current study proposes a hysteretic response curve which considers the residual deformations.

The flow chart to calculate the moment-rotation behavior of a hybrid connection is presented in Figure 1. In the first step, the gap opening angle (may also be called rotation angle, θ_c) between beam and column is imposed. Secondly a neutral axis depth, c for the crossection is assumed and the monolithic beam analogy for precast members is used to find the concrete compression fiber strain, ε_c (Equation 1 and 2).

Monolithic beam analogy claims that, if two beams, of which one was with hybrid and the other one was with monolithic connection, had identical geometry and reinforcement, the elastic deformations would be the same and, when imposing the same total displacements the plastic contributions can be equated (Pampanin et al., 2001). The plastic hinge length, l_p calculation may be done according to the approach of Paulay (Paulay and Priestley, 1992).

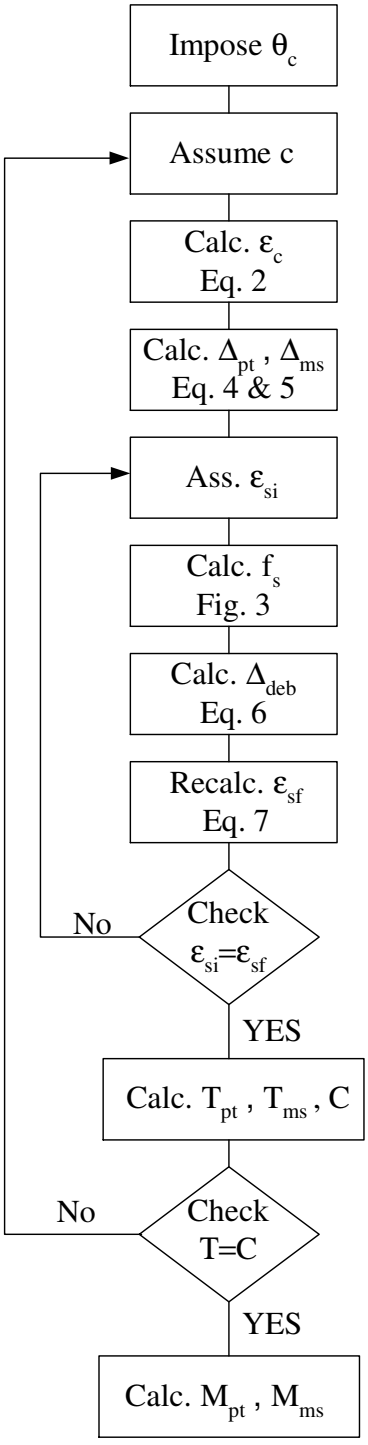

Figure 1. The algorithm for the moment-rotation behavior.

$$l_p = 0.08L_{cant} + 0.022d_b f_y \qquad (mm) \tag{1}$$

The variable L_{cant} represents the length of the cantilever and d_b and f_y are the bar diameter and yield strength of the reinforcement, respectively. The concrete strain, ε_c at the hybrid connection can be defined as:

$$\varepsilon_c = \frac{\theta_c \times c}{l_p} \tag{2}$$

The Equation 2 is a simplified illustration for the relation between the strain in concrete and the rotation at the beam-column connection. The difference between the more accurate calculation of the concrete compression fiber strain, ε_c as given in Equation 3, where ϕ_y represents the yielding curvature, and the approximate one (Equation 2) for precast members were reported as minor (Pampanin et al., 2001).

$$\varepsilon_c = \left[\frac{(\theta_c \times L_{cant})}{\left(L_{cant} - \frac{l_p}{2}\right) l_p} + \phi_y \right] c \tag{3}$$

In the fourth step (Figure 1), the elongation at strands, Δ_{pt} and mild steel, Δ_{ms} are calculated by using similar triangles approach (Figure 2) and the Equation 4 and Equation 5.

$$\Delta_{pt} = \theta_c \left(\frac{h}{2} - c \right) \tag{4}$$

$$\Delta_{ms} = \theta_c (d - c) \tag{5}$$

where h is the beam total height and d is the effective depth of the beam.

In the fifth step (Figure 1), an assumption on the strain level of the mild steel, ε_{si} need to be done. By using Figure 3, which shows a tri-linear idealization of the mild steel, the stress on mild steel, f_s is calculated. Although other constitutive models were reported by Restrepo (1993) for the modeling of mild steel bars, a tri-linear model is chosen due to the ease of application, especially for the design engineers.

The test data on the hybrid connections (Ozden and Ertas, 2007) revealed that the elongation of mild steel was not solely related to the initially imposed unbonded length l_{un} but also the de-bonding behavior of the mild steel. When the comparisons with strain level and the elongations were made, strain penetration towards to the steel ducts was observed. In order to determine the additional debonding length, Δ_{deb}, experimental test data taken from bond tests performed in Kocaeli and Bogazici Universities were used (Akpinar, 2004; Karaduman, 1998; Tezcan, 1999; Yalcinkaya, 2004). These researches showed that the debonded length was directly related with the stress and the strain level of the mild steel.

In these tests, debonding length was increasing even if the steel was in the yield plateau. It is observed that the other factors affecting the debonding length are the concrete or grout compressive strength, f_g mild steel bar diameter, d_b and the re-bar cover thickness.

A similar approache was reported by Raynor (2002) for the bond-slip response of reinforcing bars grouted in ducts. In the currently proposed model, the debonding length of the mild steel is taken into consideration as shown in Equation 6. The cover thickness of the mild steel is not considered as a variable since the mild steels are located in steel ducts in hybrid connections. It is assumed that the

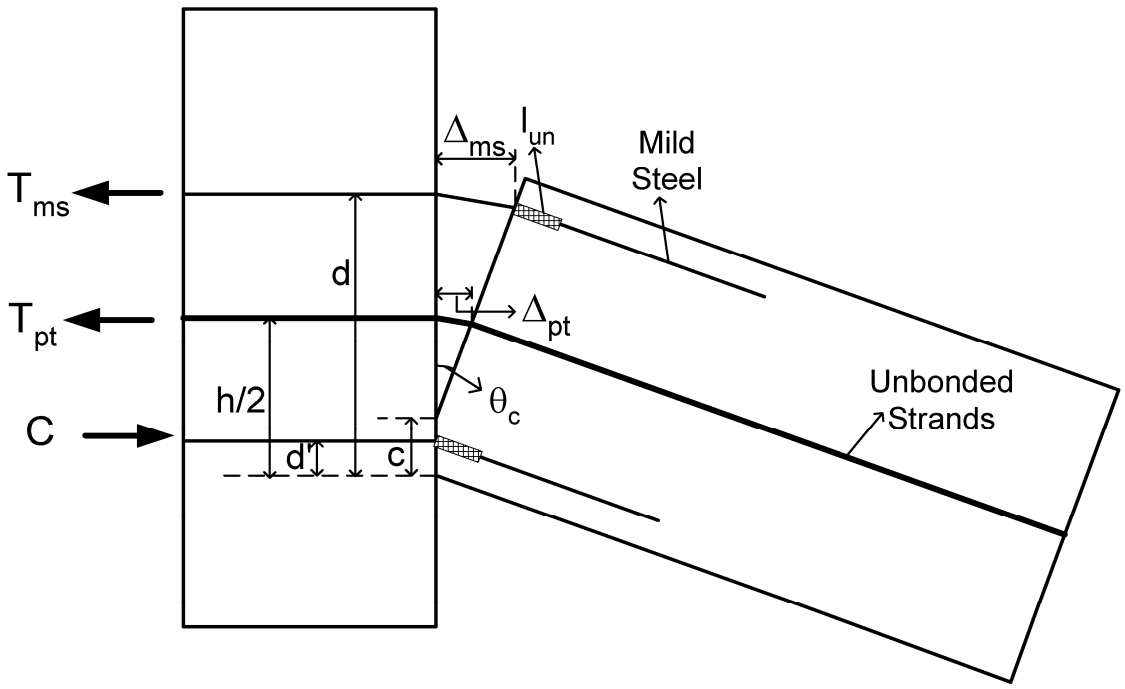

Figure 2. Schematic representation of gap opening.

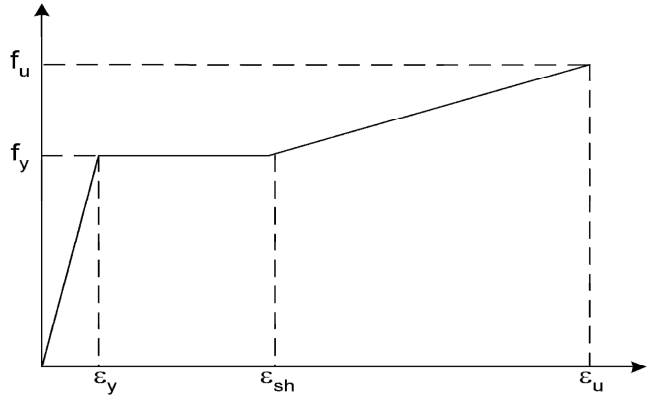

Figure 3. Idealized stress-strain behavior of mild steel.

strain penetration which takes place on both sides of the gap opening is equal; towards the beam and column.

$$\Delta_{deb} = 2\left(0.40\frac{f_s \times \varepsilon_{si} \times \sqrt{d_b}}{\sqrt{f_g}}\right) \qquad (mm) \tag{6}$$

In the following step of the procedure defined in Figure 1, the calculated final strain in the mild steel, ε_{sf} by using the Equation 7 is to be checked with the assumed initial mild steel strain, ε_{si}. Until the convergence of assumed and final strains, successive iterations are to be performed. In the next step, the force balance condition at the beam crossection, right at the gap opening section, should be checked. Initially, the strain in the strands, ε_{pt} is calculated from the Equation 8 where ε_{pi} is the initial strain due to the post-tensioning and L_{un} is the unbonded length of these strands. At this point, strain distribution along the unbonded length of the tendons is assumed uniform. After that, by using Ramberg-Osgood formulation as presented in Equation 9 for low relaxation tendons, the stress on strand, f_{pt} is calculated.

$$\varepsilon_{sf} = \frac{\Delta_{ms}}{l_{un} + \Delta_{deb}} \tag{7}$$

$$\varepsilon_{pt} = \frac{\Delta_{pt}}{L_{un}} + \varepsilon_{pi} \tag{8}$$

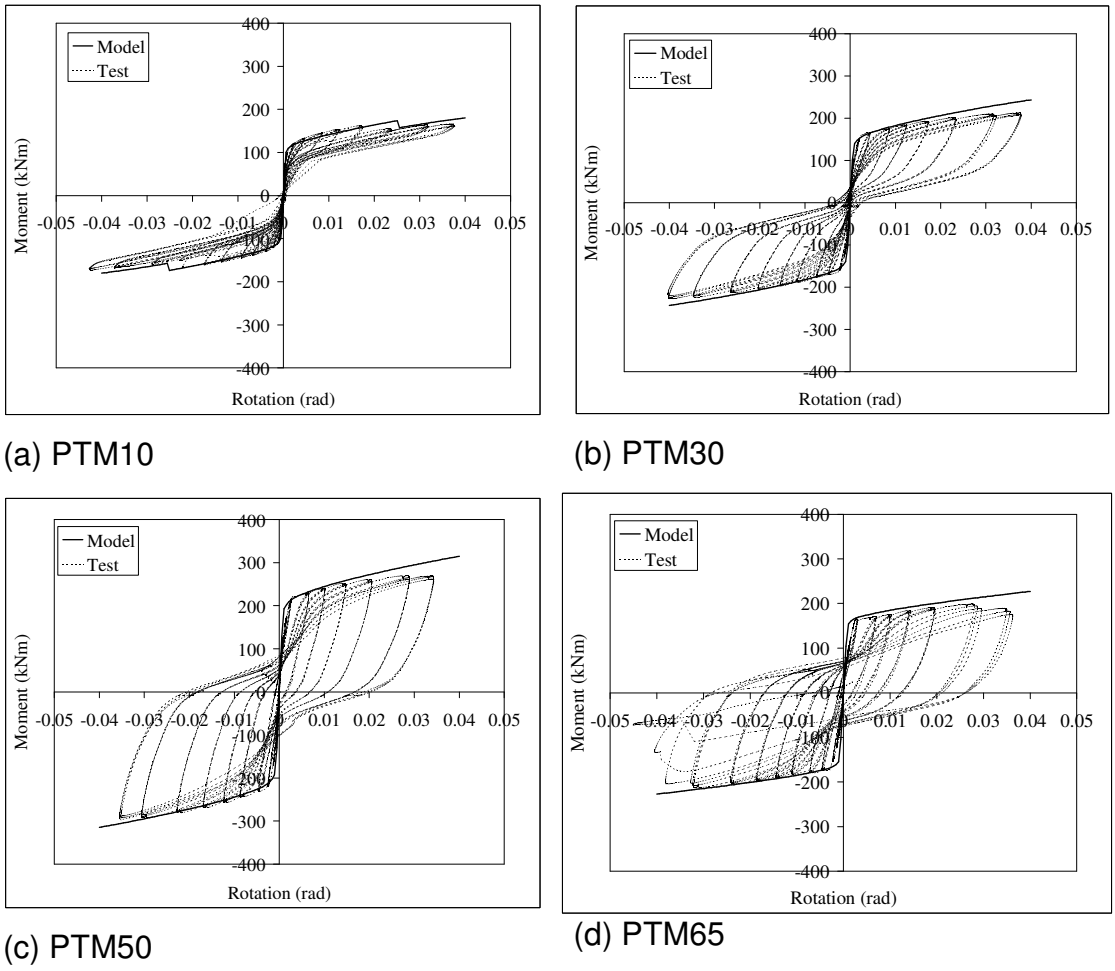

Figure 4. Comparison of test result and the proposed model for moment-rotation.

$$f_{pt} = 200\times10^{3}\varepsilon_{pt}\left\{0.025+\frac{0.975}{\left[1+\left(118\varepsilon_{pt}\right)^{10}\right]^{0.10}}\right\}\le 1860 \quad (MPa) \tag{9}$$

Mander's confined concrete model (Mander et al. (1988) is used for the confined concrete stress-strain relation since the connection region is heavily confined by high amount of rectangular closed stirrups and steel plates at the beam-column interface. These configuration generally delays the concrete crushing hence, confined concrete model is more appropriate, instead of an unconfined concrete model. The strain distribution on the compressive block is assumed linear throughout the analysis. Using this model, compression force component due to the concrete block, C_c is calculated. Until the section equilibrium condition as defined in Equation 10 is satisfied, the assumption of neutral axis depth is iterated.

$$T_{pt} + T_{ms} = C_c + C_{ms} = C \tag{10}$$

The T_{pt} and T_{ms} variables are the tension force component due to the strand and the mild steel respectively, while the variable C_{ms} is the compression force resultant due to the mild steel. When two assumptions are satisfied, the flexural moment capacity of the crossection is calculated. The relative moment contributions of the prestressing strand, M_{pt} and the mild steel, M_{ms} are computed accordingly.

Experimental Validation for Moment-Rotation Behavior

The experimental program that was performed on post-tensioned connections with different mild steel ratios yielded envelope curves of the specimens having different flexural moment contributions from the mild steel (PTM10, PTM30, PTM50, and PTM65) and the prestressing tendons. The details and the behavior of these test specimens are discussed elsewhere (Ozden and Ertas, 2007). The numbers in the names of the specimens indicates that part of the moment capacity carried by the mild steel. The comparisons on the proposed numerical approach and on these specimens in terms of moment-rotation behavior of the hybrid connection are presented in Figure 4. Generally, the numerical moment-rotation behavior coincided with the backbone curve of the experimental results. For specimen PTM10, the predicted rupture of mild steel was later than

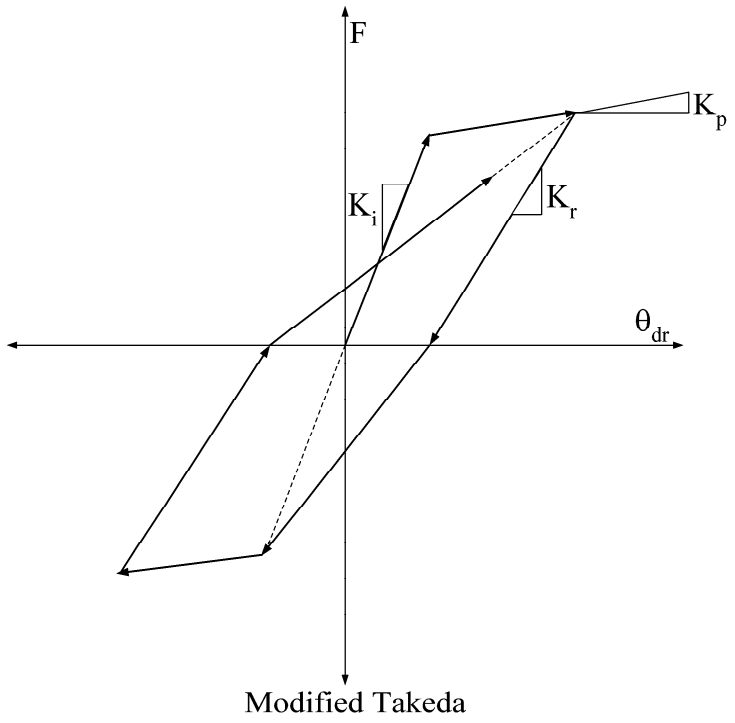

Figure 5. Modified Takeda model.

the experimental result. In specimen PTM10 a smaller mild steel diameter was used in the huge steel duct as compared to the other specimens.

Therefore, the debonded length prediction was probably longer than the experimental value. Hence the rupture of the mild steel in the simulations is delayed. The numerical response is the same as the experimental result both in elastic and inelastic region for specimens PTM30 and PTM50 with only minor difference for the ultimate flexural moment capacity at around 0.04 radians. When the predicted elastic response of PTM65 was compared with test result, numerical curve was slightly stiffer.

Cyclic modeling of beam-column subassemblies

In this part of the paper the proposed cyclic model for hybrid connections which considers the residual displacements is discussed. The experimental response curves of the specimens, with which the proposed model is compared, are reported elsewhere (Ozden and Ertas, 2007).

The hysteretic curves of the proposed model will be compared with the hysteretic curves of the specimens, along with the experimental and analytical energy dissipation curves. It is believed that the overall shape of an analytical curve may represent the overall behavior of a reversed cyclic test, and it should be better if the dissipated energies are also comparable.

Three hysteretic models, which are bilinear self-centering spring model, modified Takeda model and the flag-shaped model are considered in the establishment of the proposed hybrid connection cyclic response model with residual displacements. The bilinear self-centering spring model is suitable for representing the behavior of unbonded post-tensioned specimens of Priestley (Priestley and Tao, 1993), while the Takeda model (Takeda et al., 1970) is widely accepted for the modeling of conventional reinforced concrete frame members (Figure 5).

In the Takeda model, the variables K_i and K_p are the initial and post yielding stiffness value of the reinforced concrete members, while the variable K_r is the unloading stiffness which considers the stiffness degradation by using Equation 11. The value of γ is given as 0.3 for pure reinforced concrete members and systems (Christopoulos et al., 2003) and μ represents the displacement ductility level of the latest hysteretic response cycle.

$$K_r = \frac{K_i}{\mu^{\gamma}} \tag{11}$$

The flag-shaped hysteretic model as illustrated in Figure 6 was developed for self-centering post-tensioned structures (Christopoulos, 2002.a). In this model, the post yield stiffness ratio of Ψ and an energy dissipation coefficient of β, depending on the stress-strain behavior of the mild steel and the mild steel contribution to the flexural moment capacity are used. It is reported that the β value ranges 0 to 1.0 (Christopoulos, 2002a). Also, the clear span and the effective depth of the beam affects the post-yielding stiffness of the flag-shaped model.

Christopoulos proposed Ψ and β values as 0.10 and 0.70 respectively for a typical post-tensioned connection (Christopoulos, 2003). Flag-shaped model does not consider residual displacements inherently because of the self-centering concept of such connections. On the other hand, when mild steel content contribution for the flexural moment capacity is more than 30 per cent, excessive residual displacements were reported (Ozden and Ertas, 2007). It can be concluded that the flag-shaped hysteretic model may not be sufficient for such specimens having higher mild steel content.

The proposed model within the framework of this study can be defined as the combination of bilinear spring model and the modified Takeda model as shown in Figure 7. The first step in the

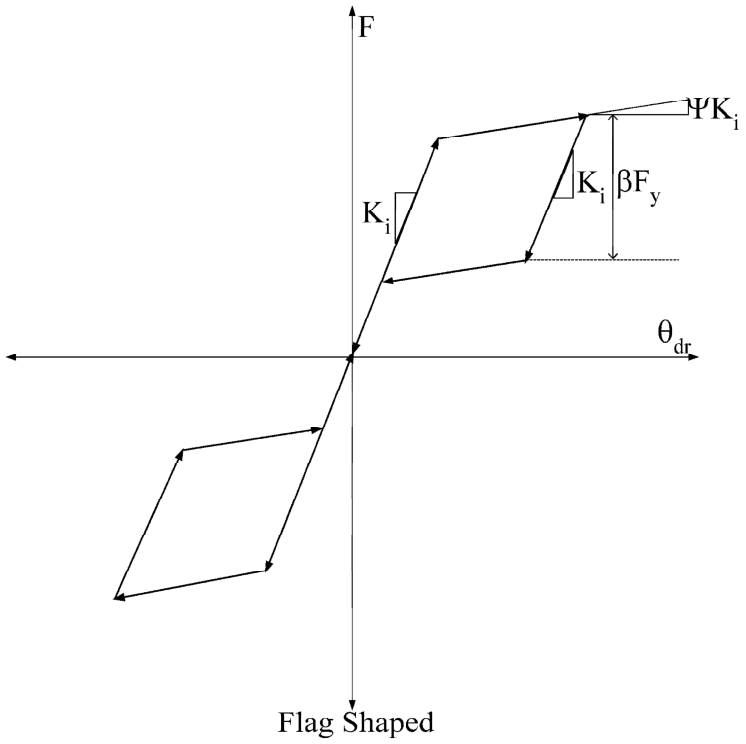

Figure 6. Flag-shaped model

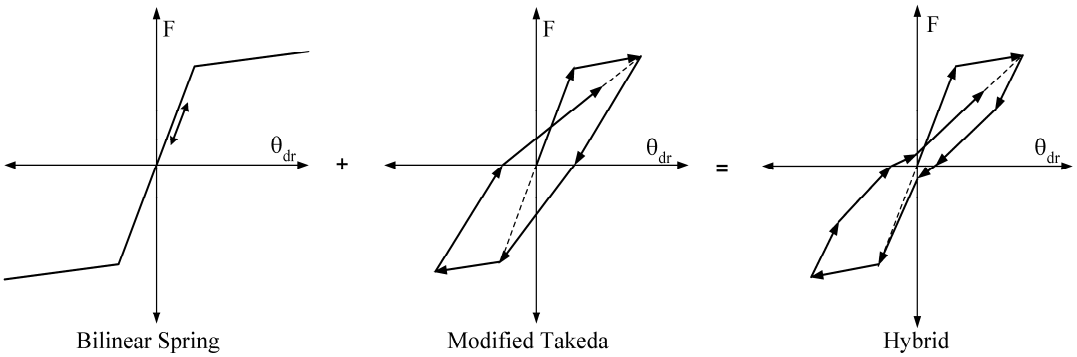

Figure 7. Components of the hybrid model.

proposed model is to calculate and draw the load-displacement backbone curve of the test subassembly as described in Figure 1. It is assumed that the nonlinear action is accumulated in the connection region for the hybrid subassemblies and the behavior of the connecting structural members are in the elastic response range. Hence, by using the virtual work theorem, that is formulated in Equation 12, lateral force, F_h and the top displacement, Δ_{top} of the column in the experimental subassembly of Ozden and Ertas (Ozden and Ertas, 2007) can easily be calculated and the lateral load-lateral displacement response can be reproduced.

$$F_h \times \Delta_{top} = M_c \times \theta_c + \int M_{beam} \times \phi_{beam} + \int M_{col} \times \phi_{col} \qquad (12)$$

where:

M_c, M_{beam}, M_{col} : Flexural moment at connection, beam and column respectively.

ϕ_{beam}□□,ϕ_{col} : The curvature value at beam and column respectively

It is observed that the cyclic response of the experimental subassemblies, successfully follows the calculated load-displacement backbone curve which is drawn by using the Equation 12 and the procedure defined in Figure 1. The response curve may be divided into two parts according to the relative contributions of the mild steel and the prestressing tendon to the flexural moment capacity of the hybrid connection. The behavior of the unbonded strand is simulated by a bilinear self-centering spring system. The remaining part of the response curve behaves like monolithic R/C members. Therefore, this type of structure is called as a partially reinforced concrete structure. The similarities of a hybrid system to a classical

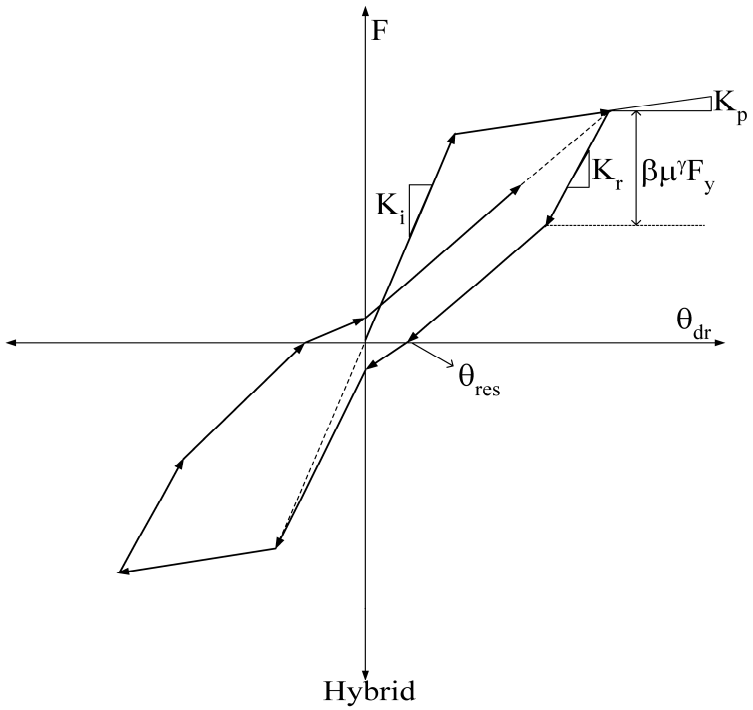

Figure 8. Presentation of the proposed hybrid model.

reinforced concrete one is directly related to the level of mild steel content at the connection. Such relation is derived from the test results (Ozden and Ertas, 2003) and represented with the square root of mild steel contribution to the moment capacity of the connection, ($\alpha^{0.5}$), where α value is calculated as presented in Equation 13.

$$\alpha = \frac{M_{ms}}{M_c} \tag{13}$$

In the proposed model, the loading branch of the hysteretic curve is defined as the summation of the effects of the post-tensioned and reinforced concrete parts of the connection; similar to the bilinear spring model and Takeda model respectively. The unloading branch of the analytical response is assumed similar to the flag-shaped model and the Takeda model as shown in Figure 8. The unloading stiffness is calculated similar to Takeda model but γ value is calculated based on the mild steel contribution to the flexural capacity (Equation 14).

$$\gamma = 0.3 \times \alpha^{0.5} \tag{14}$$

In Equation 14, when the mild steel contribution is 1, γ is 0.3 and this corresponds to a purely reinforced concrete structure. On the other hand, if the mild steel contribution is 0, γ is 0 and this represents a purely post-tensioned system. In the next step, the definition of the energy dissipation coefficient β will be made. By using the test results (Ozden and Ertas, 2007), depending on the mild steel content, β changes from 0.3 to 0.75 as shown in Figure 9. Again, the tests showed that, this unloading branch depends not only on the β value and the yield force level, F_y but also the displacement ductility at the current hysteretic cycle with increasing residual strain in the mild steel. Another critical point of the hysteretic curve is to define the residual displacement, δ_r or the residual story drift, θ_{res} value. Kawashima (Kawashima) reported that the 1996 Japanese seismic design code for bridges defines a variable for residual displacement, δ_r as presented in Equation 15, where δ_y is the yield displacement and c_r is a factor depending on the stiffness ratio. Based on this approach, a new residual story drift equation (Equation 16) is proposed and calibrated with the test results of Ozden and Ertas (2007). This calibration variable, λ changes from 0.1 to 1.0, depending on the mild steel content as illustrated in Figure 10. For low mild steel contribution, the calculation of residual story drift is minor or at a negligible level.

$$\delta_r = c_r \left(1 - \frac{K_p}{K_i}\right)(\mu - 1)\delta_y \tag{15}$$

$$\theta_{res} = \lambda \alpha^{0.5} \left(1 - \frac{K_p}{K_i}\right)(\mu - 1)\theta_y \tag{16}$$

θ_y represents the yield story drift.

The last critical point for the cyclic modeling is the lateral load value at the zero story drift level. Due to the self-centering effect, pinching behavior is observed in the hybrid connection tests (Ozden and Ertas, 2007). When the story drift is zero, the contribution of the prestressing strand to the connection moment is zero because of the bilinear model. As a result, the lateral load is directly calculated from the Takeda model with sole mild steel contribution.

Verification of the Proposed Model

Four different hybrid connections tested by Ozden and Ertas (2007) are used to verify the currently proposed hysteretic response

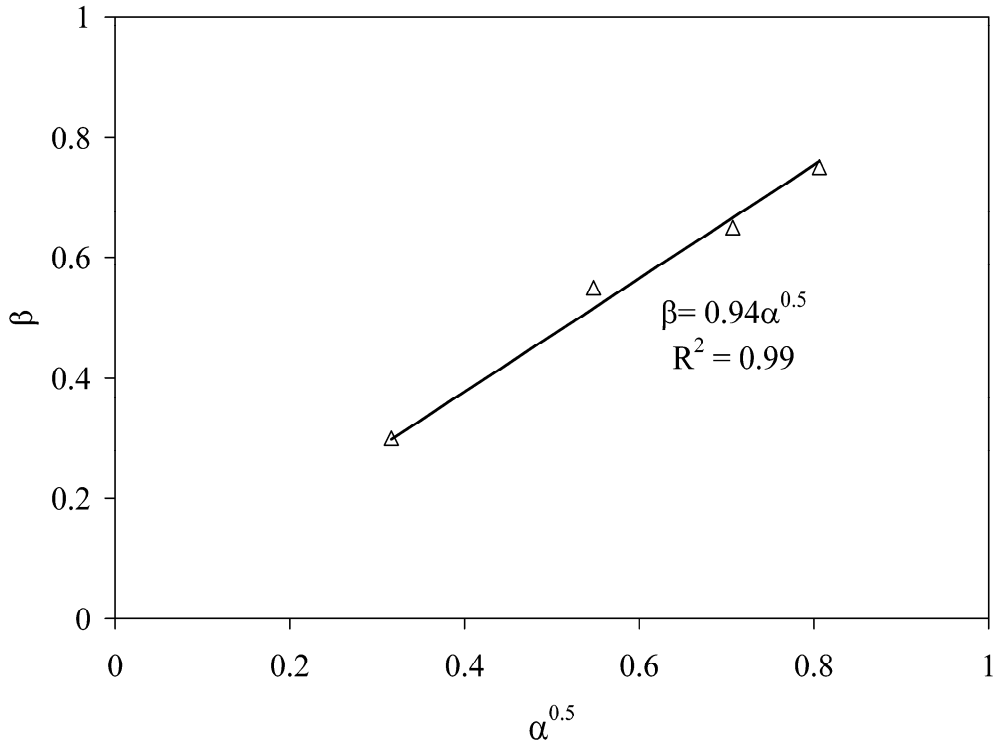

Figure 9. Calibration of the energy dissipation coefficient, β.

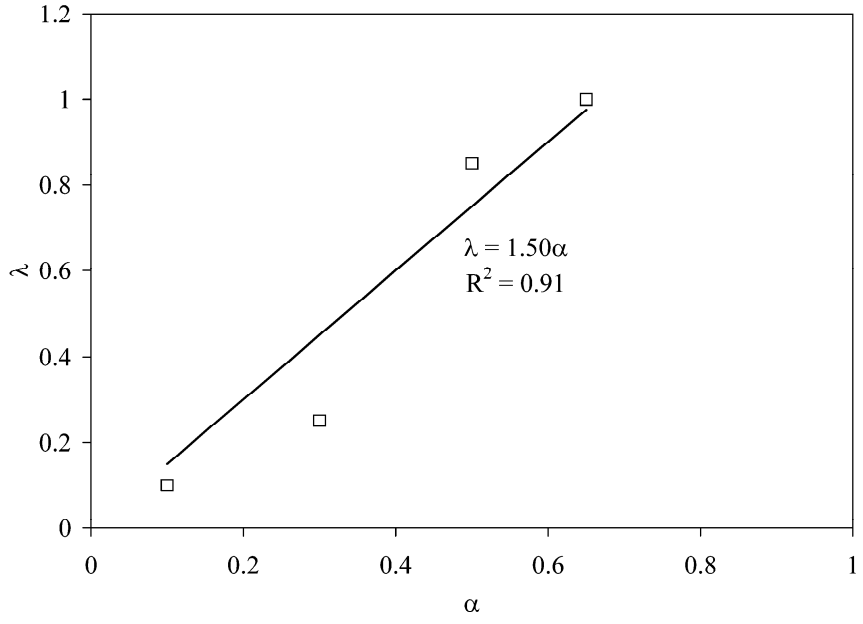

Figure 10. Residual displacement coefficient, λ.

model. Briefly, the overall behavior of the numerical studies show good agreement with the test results at initial loading, unloading and reloading parts of the response curve. In the test results, the behavior of forward and backward cycles were not symmetrical therefore, the current model results generally coincided with the backward cycle as shown in Figure 11. For PTM10, the proposed model yields good estimation up to the rupture of mild steel. After that point, the system behavior is simulated with the bilinear spring model. The correlation between the experimental results and the predicted response of specimens PTM30 and PTM50 yielded that the proposed model has good estimations on residual story drifts and self-centering effects. Although the behavior of PTM65 was

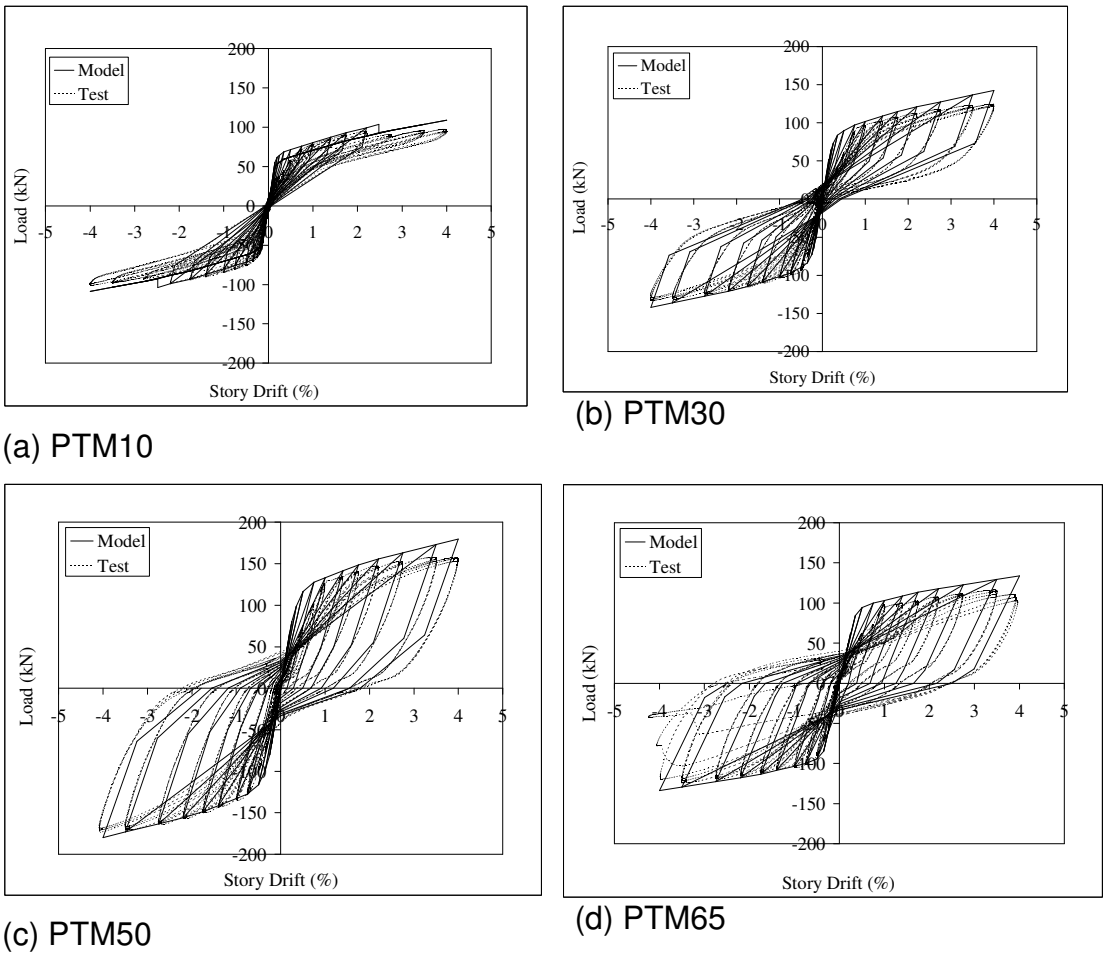

Figure 11. Verification of hysteretic model with test result of Ozden and Ertas (2007).

widely similar to the monolithic behavior, the model also predicts the specimen PTM65 relatively good. Another comparison is done according to the cumulative energy dissipation values of the specimens as presented in Figure 12.

Loading cycles were repeated three times at each story drift level during the test hence energy dissipation values for the specific story drift level is calculated by taking the average of cumulative value of these three cycles and compared with the analytical results. The energy performance values of numerical model and the test results are identical with negligible errors except PTM10.

Until the rupture of mild steel in PTM10, the energy dissipation values of the model and the test resulted very similar values. After that point, due to the bilinear self-centering model, there was no additional energy dissipation at the connection and error in predictions is observed. For the rest of the specimens the energy dissipation values of numerical and experimental works yielded very good correlations.

It should be noted that the above verifications may be considered valid for the real structures only with the assumption that the torsional deformations, either due to the existence of one-way precast slabs or due to the non-orthogonal earthquake excitations are negligible, as it is the same for the previously proposed models.

DISCUSSION and CONCLUSIONS

Experimental investigations on precast hybrid, and conventional reinforced concrete beam-to-column connections revealed important differences especially under reversed cyclic loading. Most of the reported data on precast hybrid connections are on two-dimensional (2-D) frames with in-plane loading. Very limited number of data is available on three-dimensional (3-D) frames of which the beams experience all degrees of freedom. It is believed that the response of 3-D frames with lateral loads on two orthogonal directions deserve further investtigation. Moreover the available analytical procedures may need modifications for such frames and loadings. Besides, the deformations imposed on the connections and on the reinforcement passing the plane of connection under different beam moment-to-shear ratios also needs experimental verifications.

Based on the comparisons with proposed model and

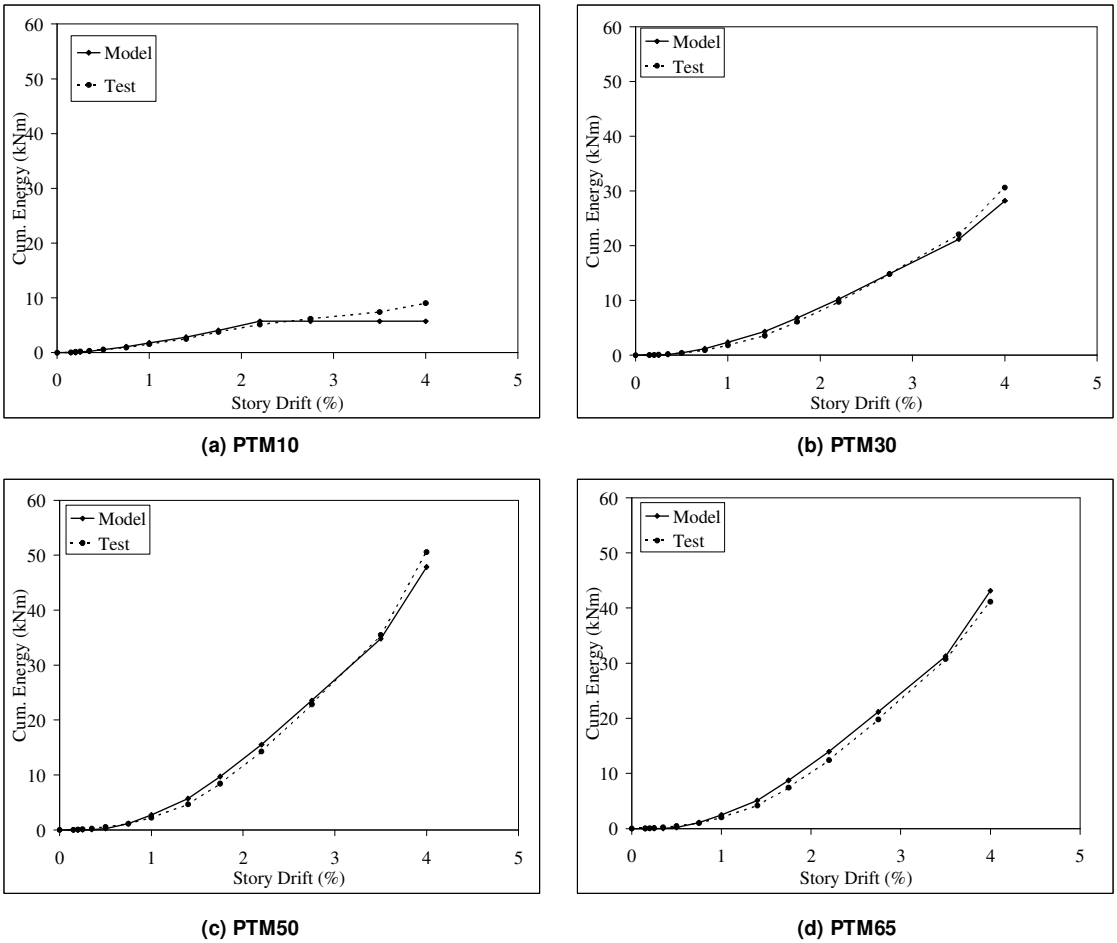

Figure 12. Comparison of experimental and analytical energy dissipations (tests from Ozden and Ertas, 2007).

the test results (Ozden and Ertas, 2007) for the unbonded post-tensioned connections with mild steel, following conclusions may be drawn:

The proposed moment-rotation modeling showed good correlation with the test results. As a result, the proposed calculation algorithm and the proposed simulation of bond-slip behavior may be applicable for the response predictions of hybrid connections with different levels of mild steel contribution.

The combination of the bilinear self-centering model and the Takeda model in order to develop the proposed hybrid model has very good agreement with the test results. Energy dissipation coefficient is directly related with the square root of the mild steel contribution for the flexural response. The similar approach may be concluded for the residual drifts. It is observed that, there is a linear relation between the permanent deformation coefficient and mild steel contribution.

It is observed that, for a specific load cycle in the post-tensioned connection specimens, the unloading stiffness value and energy dissipation characteristics and permanent deformations are dependent on displacement ductility ratio of this level.

Hysteretic model behavior demonstrated similar results with the experimental ones. The estimation of residual drift coincided with the test results. Furthermore, the cumulative energy dissipation values are very similar to the experimental values for all specimens.

The proposed hysteretic response model may well be used to predict the nonlinear response of hybrid connections as well as the nonlinear response of the overall precast concrete frame structures with hybrid connections.

REFERENCES

ACI T1.2-03 (2003). Special Hybrid Moment Frames Composed of Discretely Jointed Precast and Post-Tensioned Concrete Members, ACI 2003.

Akpınar E (2004). Upgrading the Bond Strength of Rebars Embedded in Normal Strength Concrete by CFRP Confinement. MS Thesis, Civil Engineering Department of Kocaeli University, Kocaeli, Turkey.

Cheok GS, Stone WC, Kunnath SK (1998). Seismic Response of Precast Concrete Frames with Hybrid Connections, ACI Struct. J. V.,

95: 527-539.
Christopoulos C, Filiatrault A, Folz B (2002a). Seismic Response of Self-centering Hysteretic SDOF Systems, Earthquake Engineering and Structural Dynamics, V.31: 1131-1150.
Christopoulos C, Filiatrault A, Uang CM, Folz B (2002b). Posttensioned Energy Dissipating Connections for Moment-Resisting Steel Frames, J. Structural Eng. ASCE, V.128: 1111-1120.
Christopoulos C, Pampanin S, Priestley MJN (2003). Performance-Based Seismic Response of Frame Structures Including Residual Deformations Part I: Single-Degree of Freedom Systems, Journal of Earthquake Engineering, V.7: 97-118.
El-Sheikh M, Pessiki S, Sause R, Lu LW (2000), Moment Rotation Behavior of Unbonded Post-Tensioned Precast Concrete Beam-Column Connections. ACI Structural Journal, V.97: 122-131.
El-Sheikh M, Sause R, Pessiki S, Lu LW (1999). Seismic Behavior and Design of Unbonded Post-Tensioned Precast Concrete Frames, PCI Journal, V.44: 54-71.
Karaduman C (1998). An investigation on anchorage bond properties of reinforcement in high-strength concrete. MS Thesis, Civil Engineering Department of Bogazici University, Istanbul, Turkey.
Kawashima K (1996). The 1996 Japanese seismic design specifications of highway bridges and the performance based design. Proceedings, Seismic Design Methodologies for the Next Generation of Codes, Balkema, Rotterdam. 371-82.
Kunnath SK, Reinhorn AM, Lobo RF (1992). IDARC Version 3.0: A program for the Inelastic Damage Analysis of RC Structures. Technical Report NCEER-92-0022, National Center for Earthquake Engineering Research, State University of New York at Buffalo.
Kurama Y (2000). Seismic Design of Unbonded Post-Tensioned Precast Concrete Walls with Supplemental Viscous Damping, ACI Structural Journal, V.97: 648-658.
Kurama Y (2001). Simplified Seismic Design Approach for Friction-Damped Unbonded Post-Tensioned Precast Concrete Walls, ACI Structural Journal, V.98: 705-716.
Kurama Y, Sause R, Pessiki S, Lu LW (1999). Lateral Load Behavior and Seismic Design of Unbonded Post-Tensioned Precast Concrete Walls, ACI Structural Journal, V.96: 622-632.
Kurama YC (2002). Hybrid Post-Tensioned Precast Concrete Walls for Use in Seismic Regions, PCI Journal, V.47: 36-58.
Kwan WP, Billington SL (2003). Unbonded Post Tensioned Concrete Bridge Piers I: Monotonic and Cyclic Analyses. Journal of Bridge Engineering, *ASCE*, 8: 92-101.
Mander JB, Priestley MJN, Park R (1988). Theoretical Stress-Strain Model for Confined Concrete, Journal of Structural Engineering, ASCE, V.114: 1804-1826.
Nakaki SD, Stanton JF, Sritharan S (1999). An overview of the PRESSS Five-Story Precast Test Building, PCI Journal, V.44: 26-39.
Ozden S, Ertas O (2007). Behavior of Unbonded, Post-Tensioned, Precast Concrete Connections with Different Percentages of Mild Steel Reinforcement, PCI Journal, V.52: 32-44.
Pampanin S, Priestley MJN, Sritharan S (2001). Analytical Modeling of the Seismic Behavior of Precast Concrete Frames Designed with Ductile Connections, Journal of Earthquake Engineering, V.5: 329-367.
Paulay T, Priestley MJN (1992). Seismic Design of Reinforced Concrete and Masonry Buildings, John Wiley and Sons Inc., New York.
Prakash V, Powell G, Campell S (1993). DRAIN-2DX Base Program Description and User Guide; Version 1.10. Report No. UCB/SEMM-93/17&18, Structural Engineering Mechanics and Materials, University of California, Berkeley.
Priestley MJN, Sritharan S, Conley J, Pampanin S (1999). Preliminary Results and Conclusions from the PRESSS Five-Story Precast Concrete Test Building. PCI Journal, V.44: 42-67.
Priestley MJN, Tao JR (1993). Seismic Response of Precast Prestressed Concrete Frames with Partially Debonded Tendons, PCI Journal, V.38: 58-69.
Priestly MJ, MacRae GA (1996). Seismic Tests of Precast Beam to Column Joint Subassemblages with Unbonded Tendons, PCI Journal, V.41: 64-80.
Raynor DJ, Lehman DE, Stanton JF (2002). Bond-Slip Response of Reinforcing Bars Grouted in Ducts, ACI Structural Journal, V.99: 568-576.
Restrepo JI (1993). Seismic Behavior of Connections between Precast Elements. Ph.D. Dissertation, Department of Civil Engineering, University of Canterbury, Christchurch, New Zealand.
Ricles JM, Sause R, Garlock MM, Zhao C (2001). Posttensioned Seismic Resistant Connections for Steel Frames. Journal of Structural Engineering, *ASCE*, V.127: 113-121.
Ricles JM, Sause R, Peng SW, Lu LW (2002). Experimental Evaluation of Earthquake Resistant Posttensioned Steel Connections. Journal of Structural Engineering, ASCE, V.128: 850-859.
Stone WC, Cheok GS, Stanton JF (1995). Performance of Hybrid Moment-Resisting Precast Beam-Column Concrete Connections Subjected to Cyclic Loading. ACI Structural Journal, V.91: 229-249.
Takeda T, Sozen M, Nielsen NN (1970). Reinforced Concrete Response to Simulated Earthquakes. Journal of Structural Division, ASCE, V.96: 2557-2573.
Tezcan J (1999). Anchorage behavior of reinforcement in high strength concrete under load reversals. MS Thesis, Civil Engineering Department of Bogazici University, Istanbul, Turkey.
Yalcinkaya O (2004). Bond fatigue behavior of reinforced high strength concrete under cyclic loading. MS Thesis, Civil Engineering Department of Bogazici University, Istanbul, Turkey.